ASF News & Notes

Fall 2014, Volume 10:2

Special Issue: Seven research highlights from the ASF SAR DAAC* User Working Group

ASF News & Notes is the Alaska Satellite Facility newsletter, published on the ASF website and by email. To receive ASF News & Notes by email or to suggest content, please contact ASF User Support, uso@asf.alaska.edu, 907- 373-6166.

Zhong Lu
Aleutian volcanoes

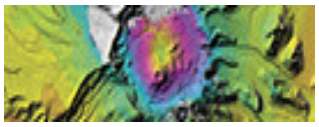

Rowena Lohman
Northwest tree heights

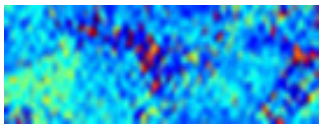

Bernd Scheuchl
Antarctica ice velocity

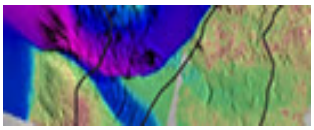

Paul Siqueira
Maine forest map

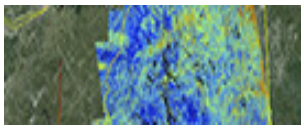

Xiaofeng Li
Hurricane morphology

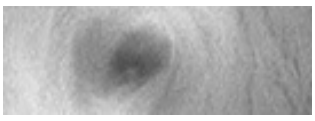

Brian D. Conway
Arizona subsidence

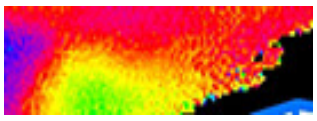

Bruce Chapman
South America wetlands

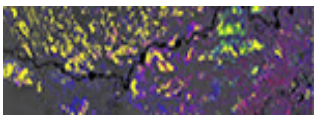

** Synthetic Aperture Radar Distributed Active Archive Center*

Insights into Aleutian Volcanism from InSAR Observations

Zhong Lu - Southern Methodist University
Dan Dzurisin - U.S. Geological Survey

Conceptual models of the magma plumbing systems and behaviors of many volcanoes in the Aleutian arc have been made possible by combining interferometric synthetic aperture radar (InSAR) data with information from the geologic record, accounts of historical eruptions, and data from seismology, petrology, gas geochemistry, and other sources.

With its global coverage, all-weather imaging capability and unprecedented spatial resolution, InSAR has become an important technique for studying magma dynamics in remote regions.

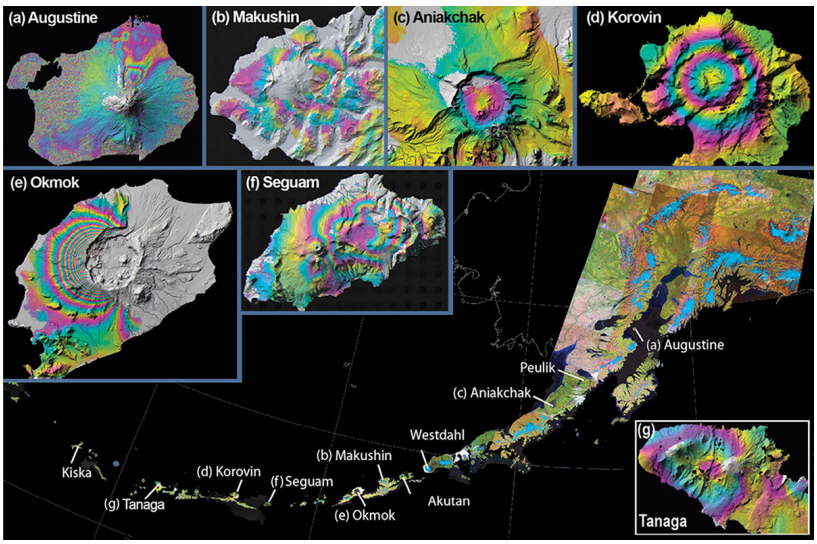

InSAR images from ERS-1, ERS-2, RADARSAT-1, and Envisat data show deformation of selected Aleutian volcanoes1: Augustine with compaction of 1986 and 2006 pyroclastic flow deposits; Makushin with ~ 7 cm of surface uplift associated with a 1995 eruption; Aniakchak with caldera subsidence at ~ 10 mm/year; Korovin exhibiting more than 6 cm of inflation in 2006; Okmok with deflation of over 50 cm during the first 13 hours of the 2008 eruption; Seguam with surface uplift of more than 6 cm from 1999 to 2000; and Tanaga with more than 5 cm of inflation during the 2005 seismic swarm. Landsat-7 image mosaic provided by S. Smith of Alaska Volcano Observatory. ©ESA 1992-2010, CSA 2004-2005, NASA.

To study Aleutian volcanism, we processed nearly 12,000 SAR images, most of which were provided by ASF, acquired by ERS-1, JERS-1, ERS-2, Radarsat-1, Envisat, ALOS, and TerraSAR-X from the early 1990s to 2010.

We combined these images to produce about 25,000 interferograms, which were analyzed for evidence of surface deformation at most of the arc's Holocene volcanoes. Where surface displacements were sufficiently strong, we used analytical models to estimate the location, shape, and volume change of deformation1.

We summarized that these processes include: (1) time-variant volcanic inflation and magmatic intrusion,

(2) deformation preceding and accompanying seismic swarms, (3) persistent volcano-wide subsidence at calderas that last erupted tens of years ago, (4) episodic magma intrusion and associated tectonic stress release, (5) subsidence from a decrease in pore-fluid pressure in active hydrothermal systems, (6) subsidence of surface lava and pyroclastic flows, and (7) no deformation at some frequently erupting volcanoes where deformation might be expected. Among the inferred mechanisms are magma accumulation in and withdrawal from crustal magma reservoirs, pressurization/depressurization of hydrothermal systems, and thermoelastic contraction of young lava or pyroclastic flows. This work demonstrates that deformation patterns and associated magma supply mechanisms at Aleutian volcanoes are diverse and vary in both space and time.

Finally, we compared the InSAR observations from the Aleutians with those from the Andes and Indonesia to highlight similarities and differences between volcanic arcs.

[1]Lu, Z., & Dzurisin, D. (2014). InSAR Imaging of Aleutian Volcanoes Monitoring a Volcanic Arc from Space (Aufl. 2014 ed.). Berlin, Heidelberg: Springer Berlin Heidelberg.

ALOS-Based Constraints on Tree Heights in the Pacific Northwest

Rowena Lohman, Veronica Prush - Department of Earth and Atmospheric Sciences, Cornell University

Our team explored the use of ALOS PALSAR data in developing a potential proxy for biomass in the Pacific Northwest[1] (Figure 1). The Pacific Northwest, with its high rates of precipitation, tall trees[2,3], and steep relief, presents challenges to the use of interferometric synthetic aperture radar (InSAR). It is also home to dense population centers, industries ranging from fishing to technology to logging, and associated hazards from landslides, earthquakes, and volcanism.

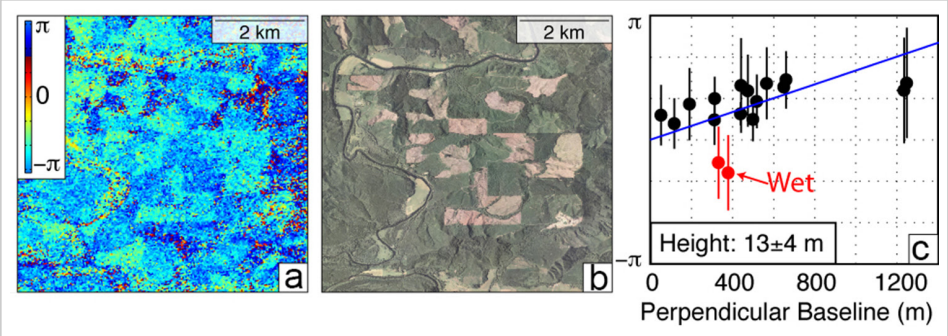

Figure 1: Small region in one interferogram (a) showing rectilinear pattern of clearcuts, visible in optical imagery (b). (c) Phase change in bare regions vs. perpendicular baseline (black dots, error bounds), has a slope proportional to the inferred height of phase scattering center height (blue line); red dots indicate interferograms with rainfall within six hours before SAR acquisitions. InSAR image © JAXA/METI 2009.

We examine InSAR time series covering the region, focusing on variations in the height of the phase-scattering center between areas with tall trees and bare ground where logging occurred (Figure 1a,b). Focusing on short spatial scales between these two area types minimizes the contributions from the atmosphere and orbital errors (which have larger spatial scales). The linear relationship (Figure 1c) between the interferometric phase change between the clearcut and surrounding trees and the perpendicular baseline of each interferogram has a slope proportional to the height of the center. This approach requires accurate, time-dependent maps of the clearcuts and standing forest,

which we generate using Landsat imagery.

Several of the interferograms in our dataset violate the linear relationship between baseline and phase change across the clearcut (red dots, Figure 1c); at relatively high baselines there is essentially zero difference in interferometric phase across clearcut boundaries. Further inspection shows that these all include dates where there was heavy rainfall immediately preceding the SAR acquisition; the resulting wet ground then contributes to the returned signal. Culling those dates using data from local weather stations results in stronger constraints on heights for the phase scattering center heights within the trees – a potential proxy for biomass that can be derived from the ALOS PALSAR catalog.

1 Prush, V., and R. Lohman (2014), Forest Canopy Heights in the Pacific Northwest Based on InSAR Phase Discontinuities across Short Spatial Scales, Remote Sensing, 6(4), 3210–3226, doi:10.3390/rs6043210.

2 e.g. Kellndorfer, J., W. Walker, L. Pierce, C. Dobson, J. A. Fites, C. Hunsaker, J. Vona, and M. Clutter (2004), Vegetation height estimation from Shuttle Radar Topography Mission and National Elevation Datasets, Remote Sensing of Environment, 93(3), 339–358, doi:10.1016/j.rse.2004.07.017.

3 e.g. Lefsky, M. A. (2010), A global forest canopy height map from the Moderate Resolution Imaging Spectroradiometer and the Geoscience Laser Altimeter System, Geophys. Res. Lett., 37(15), doi: 10.1029/2010GL043622.

Ice Velocity Mapping in Antarctica

Bernd Scheuchl, Jeremie Mouginot, Eric Rignot - University of California, Irvine

Ice sheets are acknowledged by the World Meteorological Organization and the United Nations Framework Convention on Climate Change as an Essential Climate Variable. Ice velocity is a crucial geophysical parameter that can be measured using spaceborne synthetic aperture radar (SAR) data. We have produced a continent wide ice velocity map based on data acquired during theInternational Polar Year, and are now are conducting a series of regional studies analyzing data from several epochs.

On Ross Ice Shelf, our results confirm the deceleration of Mercer and Whillans Ice Streams, with a 12-year difference in speed of –16.7 % and –25.3 %, respectively. The resulting change map shows, for the first time, the entire spatial extent of the deceleration. The reduction in speed extends hundreds of km

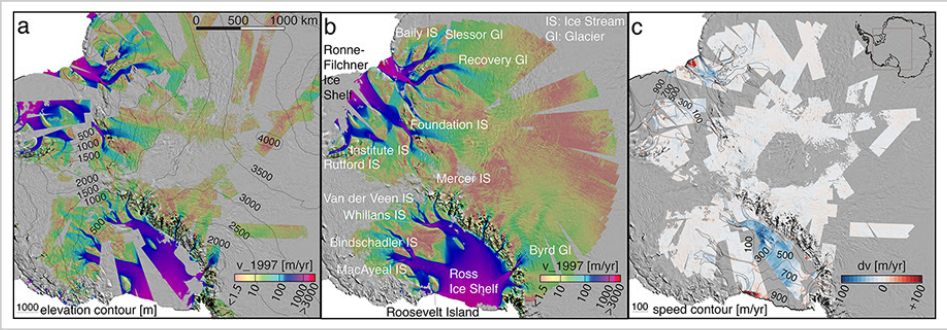

Ice-surface velocity maps for Central Antarctica for 1997 (a) and 2009 (b) overlaid on a MODIS mosaic; (c) shows the difference in speed (2009–1997) for the entire region. Blue tones indicate a deceleration, red tones an acceleration. The two dark red regions on the ice shelf edges (Ross Ice Shelf

upstream and onto the shelf.

near Roosevelt Island and Filchner Ice Shelf) indicate pre-calving. Source data © CSA 1997, 2009.

Our results contrast the relative stability of Central Antarctica with a dramatic increase in flow speed and associated mass loss in the Amundsen Sea Embayment in West Antarctica, with an increase in ice discharge (77% since 1973) into the ocean from the collective ensemble of these large glaciers. During retreat across their respective ice plains, Pine Island and Smith Glaciers underwent a rapid increase in ice discharge. However, since 2009, the ice discharge of Pine Island has remained steady. Thwaites Glacier, which had experienced a steady flow since 1992, started to speed up in 2006 and has increased its ice discharge considerably since. The acceleration of Thwaites Glacier more than compensated for the recent stoppage of the acceleration of Pine Island Glacier. Using differential SAR interferometry, we also measure a grounding line retreat of up to 35 km for these glaciers between 1992 and 2011.

Data analysis and Earth System Data Record production is conducted at the Department of Earth System Science, University of California, Irvine, under a contract with NASA's MEaSUREs program. The velocity maps are available atNSIDC. SAR data were made available for this project courtesy of the Polar Space Task Group.

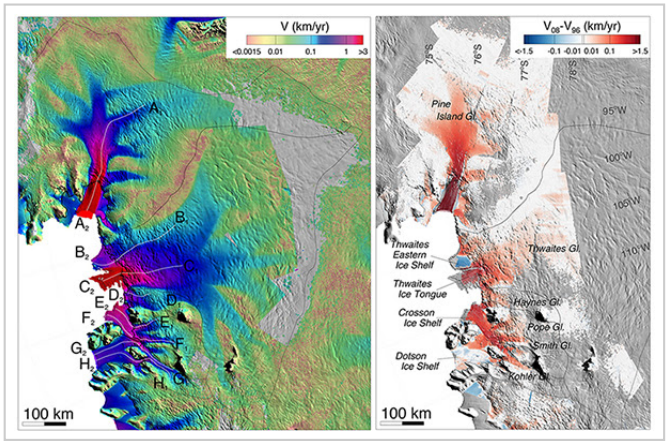

Left panel: Flow speed of the Amundsen Sea Embayment (ASE) sector of West Antarctica, color coded on a logarithmic scale and obtained combining satellite observations spanning from year 1996 to year 2013 with flux gates at the location of the grounding lines in 2011 (thick black lines) and topographic divides (thin black lines). Right panel: Change in flow speed between 2008 and 1996 color coded on a logarithmic scale and overlaid on a MODIS mosaic. Source data © ESA 1992, 1994, 1995-1996; CSA 2001-2006, 2011, 2013; JAXA/METI 2006-2011; DLR 2012, 2013.

Rignot, E., J. Mouginot, M. Morlighem, H. Seroussi, and B. Scheuchl (2014), Widespread, rapid grounding line retreat of Pine Island, Thwaites, Smith, and Kohler glaciers, West Antarctica, from 1992 to 2011, Geophys. Res. Lett., 41, 3502–3509, doi:10.1002/2014GL060140.

Mouginot, J., E. Rignot, and B. Scheuchl (2014), Sustained increase in ice discharge from the Amundsen Sea Embayment, West Antarctica, from 1973 to 2013, Geophys. Res. Lett., 41, 1576–1584, doi: 10.1002/2013GL059069.

Scheuchl, B., J. Mouginot, E. Rignot (2012), Ice velocity changes in the Ross and Ronne sectors observed using satellite radar data from 1997 and 2009, The Cryosphere 6, 1019-1030, doi: 10.5194/tc-6-1019-2012.

Rignot, E., J. Mouginot, and B. Scheuchl (2011), Ice Flow of the Antarctic Ice Sheet, Science, Vol. 333 no. 6048 pp. 1427-1430 doi: 10.1126/science.1208336.

A Forest-Height Map for the State of Maine

Paul Siqueira, Yang Lei - University of Massachusetts, Amherst

In order to create a forest-height map (Figure 1) for the state of Maine, we used 37 pairs of repeat-pass ALOS PALSAR images to relate the interferometric decorrelation signature to vegetation height.

An advantage of deriving heights from interferometric synthetic aperture radar (InSAR) is that the data can be collected autonomously using an orbiting satellite sensor such as ALOS PALSAR, and does not require additional information, such as the below-canopy topography, in order to estimate height. Heights were calibrated by using a 44,000-hectare map of heights obtained in central Maine from NASA's Land, Vegetation, and Ice Sensor (LVIS). Areas of overlap between adjacent PALSAR scenes were used to propagate the solution from the central region near the Howland Forest region (Figure 2) to the entire state.

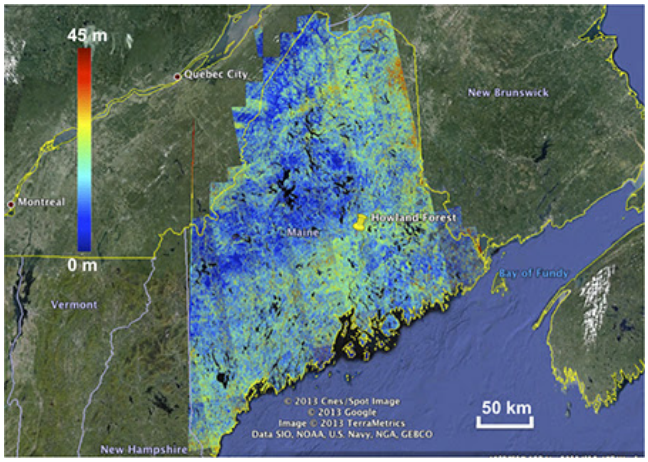

Figure 1. A 9-million-hectare mosaic of forest height for the state of Maine, constructed from repeat-pass ALOS PALSAR data obtained through the Alaska Satellite Facility's Vertex data portal. © JAXA/METI.

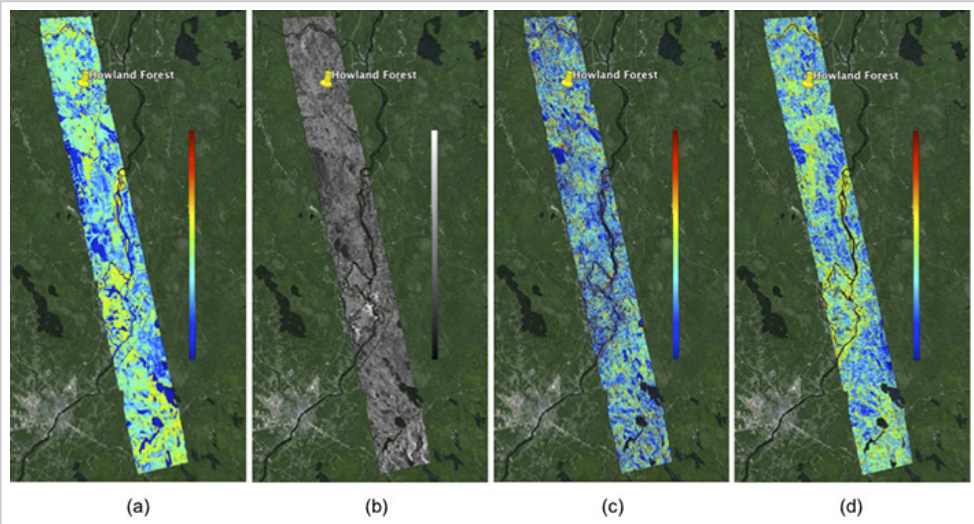

Figure 2. A closeup of the region in central Maine where LVIS data and repeat-pass ALOS PALSAR interferometric images were available. Shown in (a) is the LVIS RH100 data extending between the Howland Forest to the north and the Penobscot Forest (not labeled) to the south, (b) an image of the ALOS backscatter reflected power, a measure often used to estimate forest biomass, (c) an image revealing the consistent heights observed by ALOS PALSAR repeat-pass L-band interferometry and NASA's Shuttle Radar Topography Mission, which used C-band; and (d), an

image of forest height obtained from the ALOS PALSAR interferometric correlation magnitude. As can be seen in the set of images, the correlation-magnitude-derived height most closely compares with the LVIS-measured heights. The range of the color bar in the images above is between 0 and 45 m. © JAXA/METI.

Hurricane Morphology and Wind-Speed Climatology from SAR

Xiaofeng Li - GST at the National Oceanic and Atmospheric Administration
Frank M. Monaldo - The Johns Hopkins University, Applied Physics Laboratory

As the two examples below illustrate, SAR imagery offers a wealth of data for meteorology.

Cyclones and typhoons: Ever since the first generation of meteorological satellites in the 1960's, Atlantic tropical cyclones and their Pacific counterparts typhoons have been monitored from conventional weather-satellite sensors with passive remote-sensing instruments. Many media have published striking pictures of the cloud-top structures of tropical cyclones at kilometer spatial resolution. Since the launch of the first spaceborne synthetic aperture radar (SAR) onboard Seasat in 1978, tropical cyclones have also been observed with SAR, which penetrates clouds with active microwave radar. SAR then receives radar backscatter from the ocean surface. As a result, a SAR image shows the imprint of a tropical cyclone on the water. Examples of these sea-surface imprints are shown in Figure 1, revealing shapes of tropical cyclone eyes.

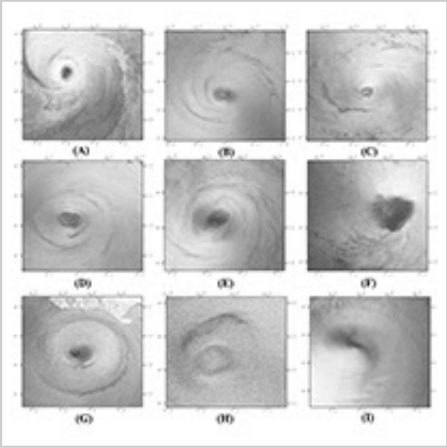

Figure 1. © CSA 2001-2007, ESA 2004-2010.

These images are from a study of sea-surface imprints of 84 hurricanes over 10 years, from 74RADARSAT-1 SAR and 10 Envisat ASAR images containing tropical cyclone signatures. Their features include eye structure, mesovortices, rain bands, and arc clouds, as well as rarities such as high winds within an eye[1] .

Wind speed: The retrieval of wind speed from SAR imagery has matured significantly over the past decade. Estimating wind speed from SAR imagery depends on the calibration of normalized radar cross section (NRCS). Soon after the launch of RADARSAT-1 in 1995, ASF began producing calibrated imagery in near real time. During the 17 years of RADARSAT-1 data, the speed and precision of processing improved. The mission's cessation offered an opportunity for ASF to re-process the data, incorporating the knowledge gained from previous processing. This reference set provided data for the analysis[2] pictured in Figure 2 of the wind-power flux density off the coasts of Delaware and Maryland, derived from over 1,400 RADARSAT-1 images.

[1] *Tropical cyclone morphology from spaceborne synthetic aperture radar - Li, X., Zhang, J. A., Yang, X. Pichel, W. G., DeMaria, M., Long, D. and Z. Li (2012),*

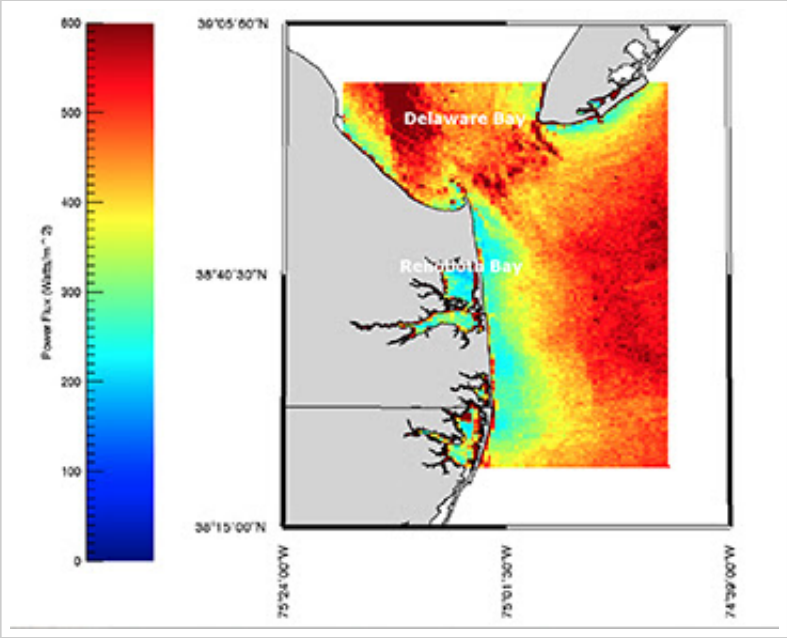

Figure 2. Wind-power flux density off the coasts of Delaware and Maryland, derived from over 1,400 RADARSAT-1 images. © CSA 2001.

94, 215-230, Bull. Amer. Meteor. Soc., doi: 10.1175/BAMS-D-11-00211.1

2 Ocean wind speed climatology from spaceborne SAR imagery - Monaldo, F. M., Li, X., Pichel, W. G. and Jackson, C. R, 2014:. Bull. Amer. Meteor. Soc., 95, 565–569. doi: 10.1175/BAMS-D-12-00165.1

Monitoring Land Subsidence and Floodplains

Brian D. Conway - Arizona Department of Water Resources

Since 2005, more than 25 land-subsidence features in Arizona, collectively covering more than 1,200 square miles of the state, have been monitored with the use of interferometric synthetic aperture radar (InSAR) data by the Arizona Department of Water Resources (ADWR). One striking example is McMullen Valley in west-central Arizona, site of both the town of Wenden and Centennial Wash, a watershed of the Gila River.

ALOS-1 PALSAR InSAR data from the Alaska Satellite Facility has been a critical resource in identifying both land subsidence in the valley and changes to the natural flow pattern around the town and the watershed. We first delineated land subsidence in the valley in 2008 with InSAR data.

In 2010, Centennial Wash flooded Wenden for the second time in 10 years. Wenden is within a land-subsidence bowl, which has exacerbated the recent flooding

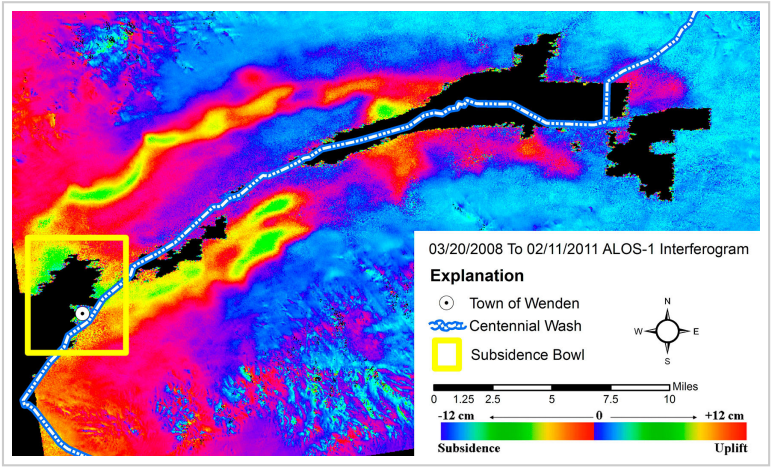

Interferogram showing subsidence between 2008 and 2011. © JAXA/METI 2008-2011.

events. The department has documented land subsidence of 2.7 feet in the center of the bowl using recent GPS survey data compared to survey data from 1991.

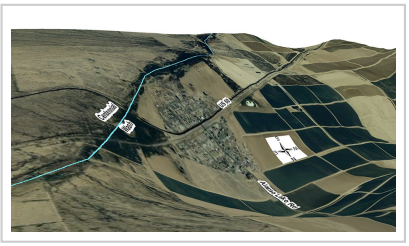

A 3-D exaggerated view of land subsidence in the town of Wenden. © ADWR 2008-2011.

The InSAR data have provided the department and floodplain managers a three-dimensional view of how the subsidence has changed the natural flow pattern around Wenden. We continue to collect InSAR data to monitor the valley.

Extent of Inundated Wetlands from ALOS SCANSAR Data

Bruce Chapman - California Institute of Technology, Jet Propulsion Laboratory
Kyle McDonald - The City College of New York

ALOS PALSAR, an orbiting L-band SAR launched by the Japanese Aerospace and Exploration Agency (JAXA) in 2006, pursued a global observation strategy through the mission's end in mid-2011. The PALSAR instrument most often operated in a subset of its available modes: fine beam HH polarization, fine beam HH and HV polarization, and SCANSAR HH. Restriction of both the mode and the look angle for many of the observations produced a time sequence of regionally consistent imagery.

The need for improved wetland characterization motivated the creation of an Inundated Wetlands Earth System Data Record (IW-ESDR) as part of NASA's Making Earth System Data Records for Use in Research Environments (MEaSUREs) program. The program has generated maps of wetland extent and inundation dynamics at two scales: 100 m, using ALOS PALSAR ScanSAR imagery; and 25 km, using multiple satellite datasets. Data inputs for IW-ESDR 100 m products were 350-km-wide ScanSAR strips acquired and processed through JAXA. These strips were calibrated, geocoded to the SRTM DEM, and assembled into regional mosaics.

Some processing of this data, particularly ortho-rectification, has been conducted on "Pleiades" at the NASA Advanced Supercomputing Division (NAS) at the NASA Ames Research Center.

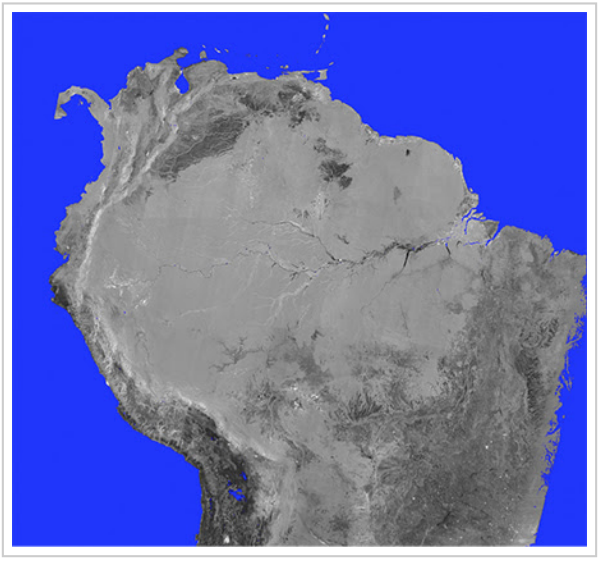

South America multi-temporal ALOS PALSAR ScanSAR image mosaic (2007-2010). This L-band HH polarization image has been radiometrically terrain corrected using the SRTM DEM. © JAXA/METI 2007-2010.

In addition to generating multi-temporal image mosaics, an

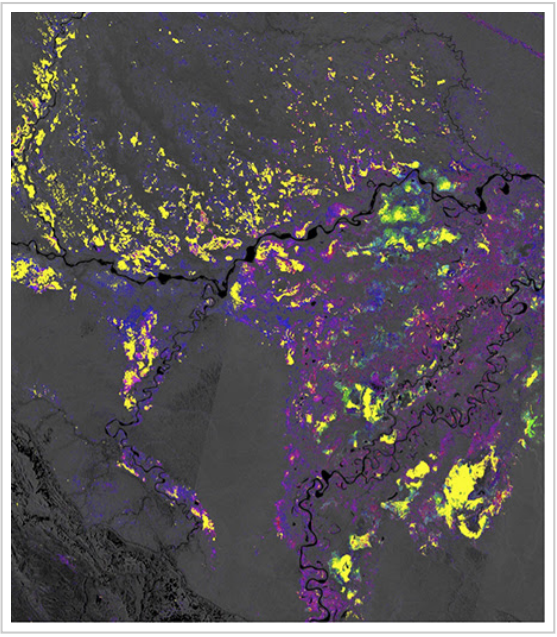

Low contrast multi-temporal image mosaic displaying inundation levels (2007) for Pacaya-Samiria reserve in Peru. Number of observations: yellow-7; light green-6; dark green-5. Number of acquisitions: turquoise-4; red-3; pink-2; dark blue-1. Dark grey indicates inundation not observed. © K&C, JAXA/METI 2007-2010.

inundation classification based on a simple image brightness threshold was generated. Examination of sequences of image classifications reveals the dynamic nature of the Pacaya-Samiria wetlands in Peru.

This research was within the framework of the ALOS Kyoto & Carbon Initiative. ALOS data were provided by JAXA EORC. Supporting resources were provided by the NASA NAS High-End Computing Program. This work was partially performed at the Jet Propulsion Laboratory, California Institute of Technology.

Copyright 2014. All rights reserved.